NRIAG Journal of Astronomy and Geophysics (2014) 3, 109–116

National Research Institute of Astronomy and Geophysics

NRIAG Journal of Astronomy and Geophysics

www.elsevier.com/locate/nrjag

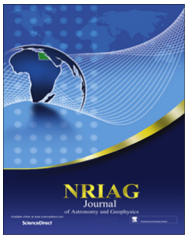

Possibility of tsunami early-warning from post-seismic ionospheric disturbance for 2 July, 2013, M_w = 6.1 Indonesia's Bireun earthquake: Two-dimensional principal component analysis

Jyh-Woei Lin *

Dept. of Earth Science, National Cheng Kung University, No. 1 University Road, Tainan City, Taiwan

Received 18 April 2014; revised 24 August 2014; accepted 25 August 2014
Available online 16 September 2014

KEYWORDS

Two-dimensional principal component analysis (2DPCA);
Two-dimensional total electron content (TEC);
Indonesia's Bireun earthquake;
Acoustic shock waves

Abstract Two-dimensional principal component analysis (2DPCA) has been used to determine ionospheric two-dimensional total electron content (TEC) anomaly after Indonesia's Bireun earthquake at 07:37:02 UT on 2 July, 2013 (M_w = 6.1). The TEC data, from 07:35 to 07:50 (UT) during the earthquake, are examined. The TEC anomaly was more intense localized at 07:40–7:45 (UT) post earthquake. Potential reason of the TEC anomaly may be an anomalous fluctuation e.g., electron density variation which is a rising high speed acoustic shock wave resulted by the mainshock of the earthquake. The duration time of the TEC anomaly was at least 5 min. The anomalous fluctuation could be an early warning for the regions far from the epicenter when it began to propagate because the tsunami arrived at the far regions much slower than the anomalous fluctuation if the tsunami was caused by an earthquake with the epicenter in the sea.

1. Introduction

Ionospheric total electron content (TEC) anomalies associated with large earthquakes have been widely researched both as precursors and aftereffects (Artru and Lognonné, 2001; Garcia et al., 2005; Hegai et al., 2006; Liu et al., 2009, 2006; Lognonné et al., 2006; Marchand and Berthelier1, 2008; Pulinets et al., 2000, 2007; Pulinets and Boyarchuk, 2004; Singh et al., 2010; Zhao et al., 2008). The exact causes of earthquake associated precursor TEC anomalies are not known; however, there are many possibilities including gravity waves generated by the solid-earth and sea, as well as lower atmospheric electric fields resulting from earthquake preparation processes that can be transferred into the ionosphere along geomagnetic lines (Pulinets, 2004). Regardless of the specific causes of earthquake-precursor TEC anomalies, their earthquake association has been established statistically

* Tel.: +886 6 2757575x65430.
E-mail address: pgjwl1966@gmail.com.
Peer review under responsibility of National Research Institute of Astronomy and Geophysics.

http://dx.doi.org/10.1016/j.nrjag.2014.08.001

using deviations from running TEC median values after eliminating other possible causes of TEC disturbance such as solar flare and geomagnetic storm activity (Lin, 2010). The TEC anomalies were most likely caused by acoustic gravity waves traveling from the earth's surface into the ionosphere (Artru and Lognonné, 2001; Garcia et al., 2005; Lognonné et al., 2006; Marchand and Berthelier1, 2008; Pulinets et al., 2000). The mechanism for this is thought to be earth's atmosphere acting as a natural amplifier. During an earthquake tiny amounts of kinetic energy are transferred from the solid earth to the lower atmosphere. If this kinetic energy is conserved, then given the exponential decline in atmospheric density with height, waves of great amplitude can result in the ionosphere. It has been estimated that millimeter disturbances at the earth's surface can be amplified to waves of amplitude 100 m at 100 km altitude (Artru and Lognonné, 2001; Lognonné et al., 2006). A study by Lognonné et al. (2006) using ground based GPS receivers to detect post-seismic ionospheric disturbance found that the measurable impact of the gravity waves resulting from the Nov. 3. Denali, Alaska $M = 7.9$ earthquake produced small but detectable changes in the TECu count of 0.1% peak to peak. This disturbance was detected by 6 other satellites. Lognonné et al. (2006) also measured the effects of near field seismic waves for the Hokkaido Tokacho–Oki earthquake on Sept. 25, 2003. In that experiment, they found that acoustic waves could be detected as high as 800 km, they also measured the gravity wave impact for the same earthquake and got similar results to those for the Alaskan Denali earthquake in terms of TECu disturbance. One issue, however, with all TEC measurement is the nature of the ionosphere. The electron content of the ionosphere is highly dynamic plasma so that establishing anomalies and event association is not easy. For example, determining a running median of TEC content before large earthquakes to search for precursor TEC anomalies is difficult and may not always be reliable because TEC can be affected by many factors. Pulinets (2004) makes an extensive list of possible causes, including radon gas release, causing lower atmospheric electric fields which travel up into the ionosphere along geomagnetic lines while Freund (2003) suggests P-type semiconductor effect as the cause of lower atmosphere electric fields. P-type semiconductor effect, whereby charge separation occurs in metamorphic, near-cracked and igneous rock between electrons in the stressed range of rock and small positive holes (p-holes) occurring away from stressed regions. Once the positive holes are generated some phenomena occur as current propagates through rocks resulting in electromagnetic emissions.

Recent studies have shown that earthquake-related TEC anomalies are detectable using principal component analysis (PCA) (Lin, 2010, 2011). PCA is an alternative pure mathematical method for measuring TEC anomalies. The method relies on exploiting signal delay between global positioning system (GPS) satellites and ground receiver stations without direct observation of ionospheric TEC. The long term period variance of ionospheric TEC (Lin, 2010) does not affect the outcome of the results using PCA and the potential influence of other factors such as solar flares and geomagnetic disturbance is eliminated using relevant Kp indexes statistically. While these PCA experiments were able to detect and even describe the spatial pattern or physical shape of earthquake-related TEC anomaly (Lin, 2011), PCA might not be as useful as two-dimensional principal component analysis (2DPCA) in the detection of TEC anomalies when applying to two-dimensional TEC data. Therefore, the goal of this study is to examine the ionospheric TEC anomaly related to Indonesia's Bireun earthquake (4.698°N, 96.687°E) at 07:37:02 UT on 2 July, 2013 ($M_w = 6.1$) with the depth of 10.0 km (U.S. Geological Survey) using 2DPCA. Possible causes of discovered anomaly will be discussed. It is expected that at the time 07:35–07:50 UT, ionospheric TEC behavior should be complicated showing large earthquake-related anomaly shortly after or during the mainshock like the results of Liu et al's work (2011) while tsunami did not occur to affect the ionosphere. The TEC data (two dimensional TEC data, F-layer) are derived using NASA Global Differential GPS system (GDGPS) and global TEC maps (GIMs) in this study are derived using TEC data from ~100 real-time GDGPS tracking sites, augmented with additional sites that are available on 5 min basis. The integrated electron density data along each receiver-GPS satellite link is processed through a Kalman filter. Processing to estimate TEC value needs to consider some biases (influences) during restoration of TEC values from measurements of dual-frequency delays of GPS signals, which related with cycle slips, resolve carrier phase ambiguity, determine hardware delays for phase, code measurements, tropospheric and multipath problems. The Kalman filter has been used to estimate the TEC with less bias (Kechine et al., 2004; Ouyang et al., 2008) (http://www.gdgps.net/system-desc/index.html).

2. Method

2.1. 2DPCA

For 2DPCA, let signals are represented by a matrix A (the dimension of $n \times m$). Linear projection of the form is considered as followed (Konga et al., 2005; Sanguansat, 2012),

$$y = Ax \tag{1}$$

Here x is an n dimensional project axis and y is the projected feature of signals on x called principal component vector.

$$S_x = E(y - Ey)(y - Ey)^T \tag{2}$$

Here S_x is the covariance matrix of the project feature vector.

The trace of S_x is defined;

$$J(x) = tr(S_x) \tag{3}$$

$$tr(S_x) = tr\{x^T G x\}, \quad \text{where } G = E[(A - EA)^T (A - EA)] \tag{4}$$

The matrix G is called signal covariance matrix. The vector x maximizing Eq. (4) corresponds to the largest (principal) eigenvalue of G, and let the largest eigenvalue be the most dominant component of the data, therefore largest eigenvalue is represented by the principal characteristics of the data (Konga et al., 2005; Sanguansat, 2012; Jeong et al., 2009). 2DPCA can be removed small sample signal size (SSS) problem for two dimensional TEC data (Fukunnaga, 1991). The PCA converts the measurements into one-dimensional data before covariance matrix calculation (Yang et al., 2004). The covariance matrix of PCA is based on an input matrix with the dimension of $m \times n$, which is reshaped from one-dimensional data (length of m multiplying n). Reshaping data will cause computing error because PCA is a tool to deal with one-dimensional data. It means that the spatial structure and

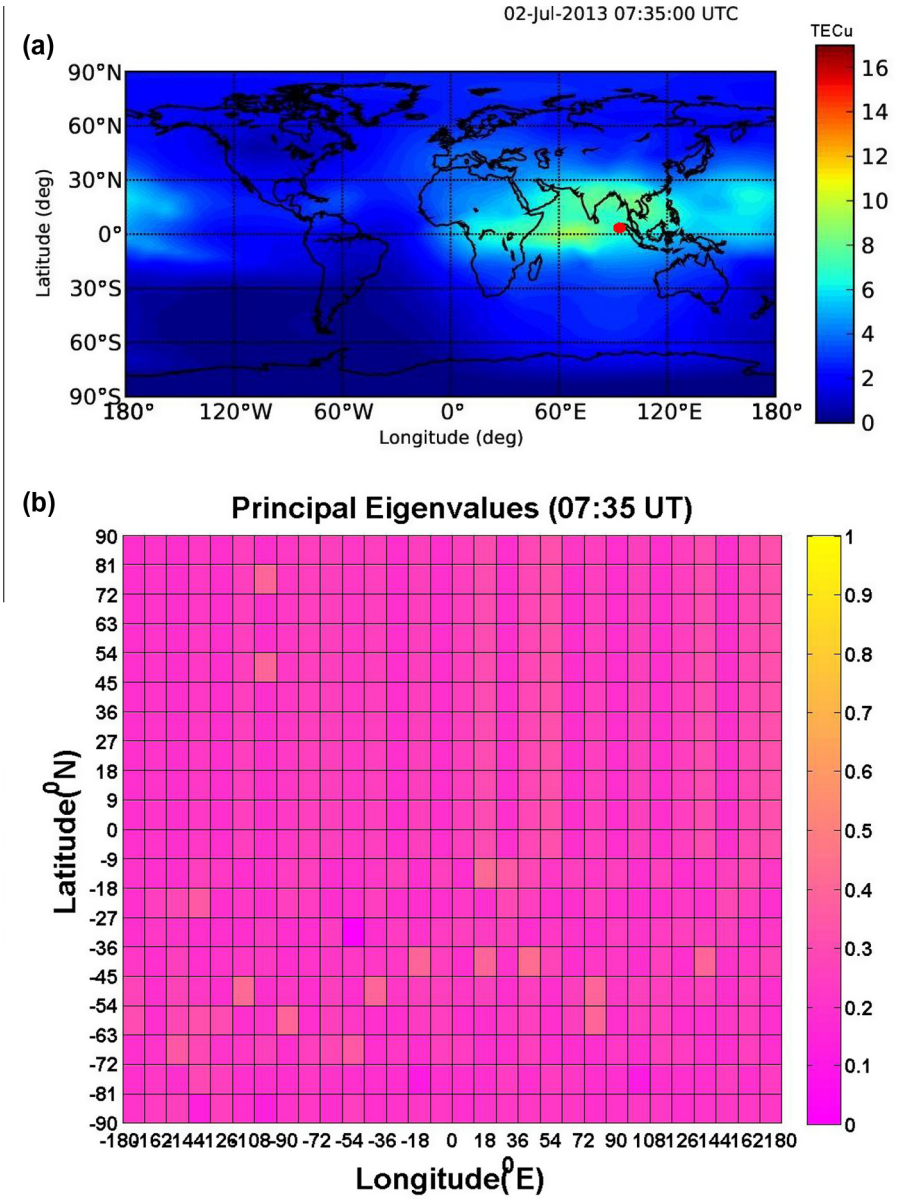

Fig. 1 (a) This figure shows the GIM at the time 07:35 UT on 2 July 2013, (b) the figure gives a color-coded scale of the magnitudes of principal eigenvalues of 2DPCA corresponding to (a). The color within an area denotes the magnitude of a principal eigenvalue corresponding to (a), so that there are 600 principal eigenvalues assigned (i.e., each area in the bottom figures represents a principal eigenvalue), respectively.

information cannot be well preserved due to some original information loss when inverting to original dimension (Kramer, 1991) under the condition of the matrix being of small sample size (SSS). Such information loss is called SSS problem. However, the covariance matrix in 2DPCA is full rank for a matrix of low dimension. Therefore the curse of dimensionality and SSS problem (low dimensional data problem) can be avoided (Konga et al., 2005; Sanguansat, 2012). TEC data are examined to detect earthquake-related TEC anomaly and GIMs are only used to observe TEC situation in this study.

2.2. TEC data processing 2DPCA

Fig. 1(a) shows the GIM at the time 07:35 UT on 2 July 2013. The earthquake-related TEC anomalies are not easy to observe using e.g. determining a running median of TEC content to detect a TEC anomaly (Liu et al., 2006). The TEC data of the global region (not dividing the GIM for image processing) in Fig. 1(a) are divided into 600 smaller areas 5° and 2.5° in longitude and latitude, respectively. The size of each small area is 12° in longitude and 9° in latitude. The spatial resolution of the TEC data for GDGPS system is 5° and 2.5° degrees in longitude and latitude, respectively (Hernández-Pajares et al., 2009; Chen and Gao, 2005; Gao and Chen, 2006) (http://www.gdgps.net/system-desc/references.html) and therefore 4 TEC data (two-dimensional data) are take in each area. The TEC were anomalies usually spread widely from the epicenters of large earthquakes from the results of Artru and Lognonné (2001), Lognonné et al. (2006) and Hobara and Parrot (2005). Therefore earthquake-related TEC anomaly is

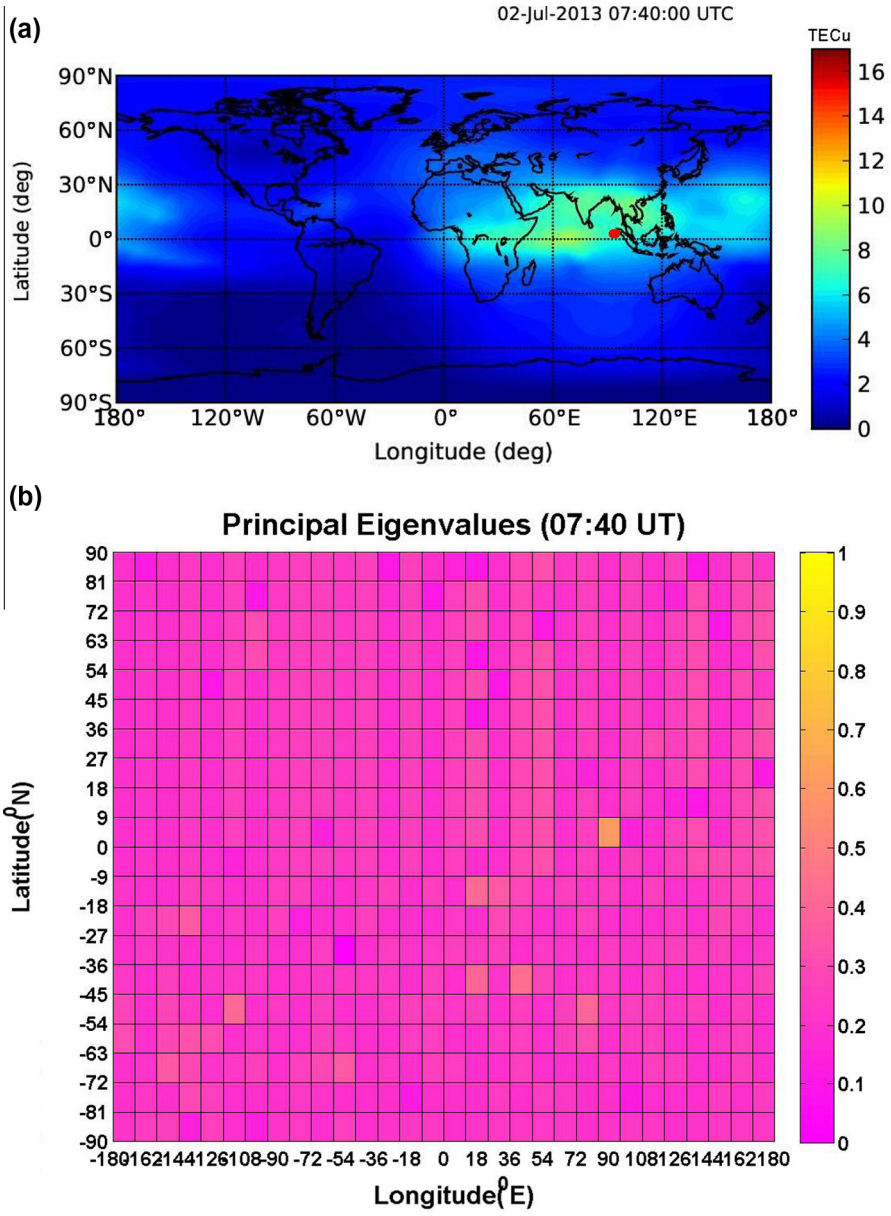

Fig. 2 (a) This figure shows the GIM at the time 07:40 UT on 2 July 2013, (b) the figure gives a color-coded scale of the magnitudes of principal eigenvalues of 2DPCA corresponding to (a).

detectable for such selected size of an area. The 4 TEC data form a matrix A of Eq. (1) with the dimensions of 2×2 as small sample signal size (SSS) in each point of Fig. 1(a). This allows for principal eigenvalues to be computed for each of the 600 smaller areas.

3. Results

The respective results are given in Fig. 1(b). The representative of large principal eigenvalues in Figs. 2(b)–4(b) shows the existence of earthquake-related TEC anomaly represented by a large principal eigenvalue at the time 07:40-07-45 UT. Non-earthquake TEC anomalies (e.g. EIA) are therefore suppressed by large principal eigenvalues defining as earthquake-related TEC anomaly. It means that if the largest principal eigenvalue related to the earthquake was taken out, then non-earthquake TEC anomalies would be clearly revealed. Therefore the TEC anomaly related to this earthquake should be very large due to its large magnitude (M_w = 6.1) and shallow depth (10.0 km). The possibility of other factors such as solar flare and geomagnetic effects affecting the results is considered by examining Kp indices (Elsner and Kavlakov, 2001; Hamilton et al., 1986; Mukherjee, 1999). July, 2 was observed as geomagnetic quiet day shown in Fig. 5 (Kp < 4).

4. Discussion

2DPCA was able to detect a TEC anomaly related to Indonesia's Bireun Earthquake at the time 07:40–07:45 UT. Identifying precise cause of earthquake related TEC anomalies is not easy. One reason for this is the number of potential causes of earthquake related TEC anomalies that arise during

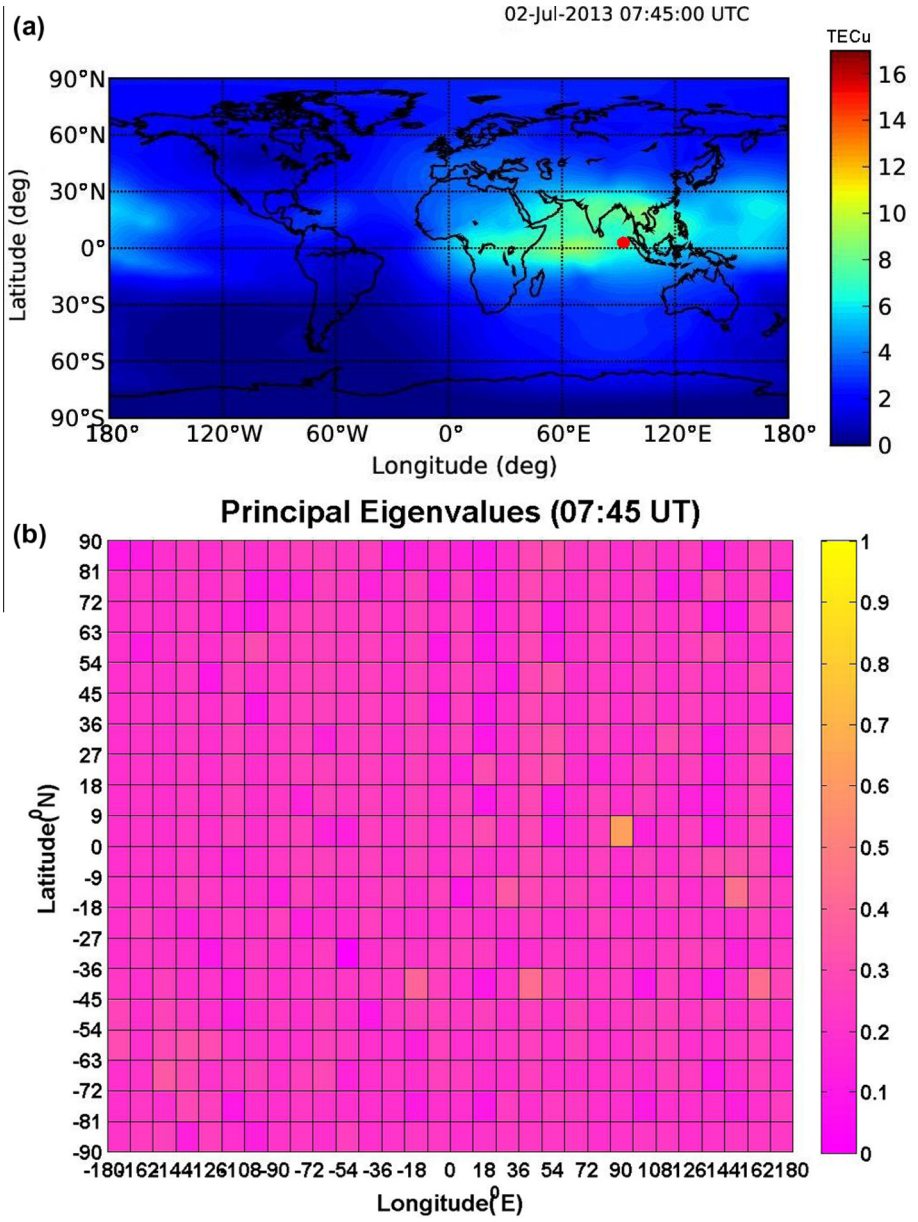

Fig. 3 (a) This figure shows the GIM at the time 07:45 UT on 2 July 2013, (b) the figure gives a color-coded scale of the magnitudes of principal eigenvalues of 2DPCA corresponding to (a).

earthquake preparation, the mainshock, and aftershocks. For example during the earthquake preparation phase, Pulinets and Boyarchuk (2004) suggested that radon emanating from active faults and cracks before earthquakes ionizes the near ground atmosphere to produce large vertical electric fields. Freund (2000) proposed that mobile positive holes in the earth's crust could be activated by low-energy impact, sound waves, and microfractures, creating charge clouds that could explain electromagnetic activity. Gravity waves arising from fine vibrations in the earth's surface leading to gas release are another possibility. This results in lower atmospheric turbulence and eventual ionospheric perturbations (Molchanov and Hayakawa, 1998). However, once an earthquake occurred, then the most evident physical mechanisms are ground motion and fine surface vibrations. Accordingly, studies of electromagnetic disturbance suggested two possible explanations for earthquake-related anomalies at this altitude. One was acoustic gravity waves caused by Joule heating (Hegai et al., 1997) and the other was the presence of an electric field creating large scale ionospheric density irregularities (Liu et al., 2004; Pulinets and Legen'ka, 2003) coupled with potential drift of the anomaly toward the equator. However, this anomaly resembled what one would expect from rising acoustic gravity waves because of strong motion. As discussed in the introduction earth's atmosphere could act as a natural amplifier due to declining atmospheric density with height. A large earthquake, such as this earthquake, was characterized by many fine vibrations at the earth's surface which could produce a vertical stark acoustic pressure wave of great amplitude by the time it reached the ionosphere.

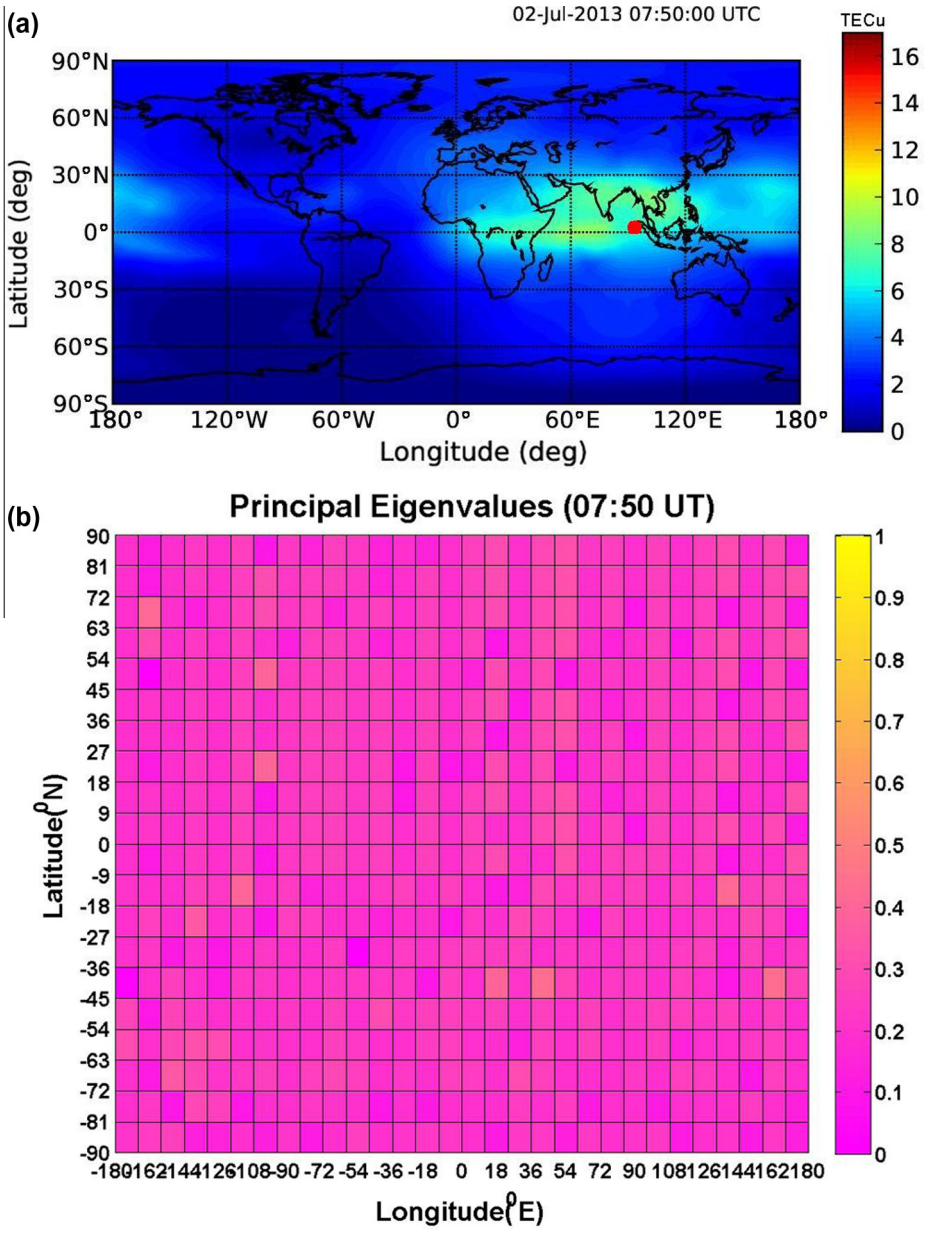

Fig. 4 (a) This figure shows the GIM at the time 7:50 UT on 2 July 2013, (b) the figure gives a color-coded scale of the magnitudes of principal eigenvalues of 2DPCA corresponding to (a).

Such a description could possibly represent the stark and concentrated energy of an acoustic shock wave being formed in the lower atmosphere after the earthquake traveling up into the ionosphere (Jin et al., 2010). This was the possibility described in the introduction to this study whereby a high speed acoustic shock wave caused by stark strong motion at the earth's surface is amplified through the atmosphere to affect an anomalous fluctuation e.g., electron density variation in the ionosphere from the earthquake zone. The duration time of earthquake-related TEC anomaly was estimated to be at least 5 min. The duration time of TEC anomaly might correlate with the damping of ionospheric plasma. The anomalous fluctuation could be an early warning for far regions when this anomalous fluctuation begins to propagate. The tsunami arrived at the far regions much slower than such anomalous fluctuation when the tsunami was caused by an earthquake with the epicenter in the sea. Afraimovich et al. (2001) researched acoustic shock waves that occur during earthquakes that affect the ionosphere. They studied the earthquake effects in Turkey on 17 August and 12 November 1999 and in Southern Sumatra on 04 June 2000 and found that the ionospheric response related to the earthquakes due to acoustic shock waves is 180–390 s. Compared with the result of this study, 2DPCA has shown its advantage and credibility to estimate the duration time of earthquake-related TEC anomaly.

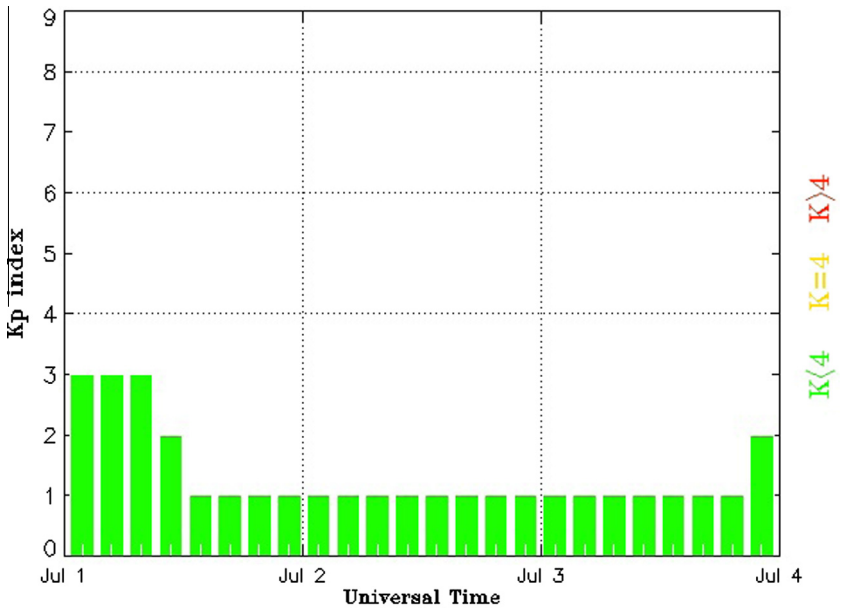

Fig. 5 Shows the Kp indices from 1 July to 3 July 2013.

5. Conclusion

2DPCA had the advantage to detect the TEC anomaly related to the 2, July 2013 Indonesia's Bireun Earthquake. Results have shown that a local ranging TEC anomaly was detectable at the time 07:40–07:45 UT. The earthquake-related TEC anomaly could be indicative of a rising high speed acoustic shock wave that might cause a TEC anomalous fluctuation e.g. density variance. The duration time of the TEC anomaly was at least 5 min. The anomalous fluctuation could be an early warning for far regions when this anomalous fluctuation was propagating.

Acknowledgments

The author is grateful to: NASA Global Differential GPS system (GDGPS) for useful Data.

References

Afraimovich, E.L., Perevalova, N.P., Plotnikov, A.V., Uralov, A.M., 2001. The shock-acoustic waves generated by earthquakes. Ann. Geophys. 19, 395–409.

Artru, J., Lognonné, P., 2001. Normal modeling of post-seismic ionospheric oscillations. Geophys. Res. Lett. 28 (4), 697–700.

Chen, K., Gao, Y., 2005. Real-time precise point positioning using single frequency data. In: ION GNSS 2005, Long Beach, CA, USA.

Elsner, J.B., Kavlakov, S.P., 2001. Hurricane intensity changes associated with geomagnetic variation. Atmos. Sci. Lett 2 (1–4), 86–93. http://dx.doi.org/10.1006/asle.2001.0040.

Freund, F., 2000. Time-resolved study of charge generation and propagation in igneous rocks. J. Geophys. Res. 105, 11001–11019.

Freund, F.T., 2003. Rocks that crackle and sparkle and glow strange pre-earthquake phenomena. J. Sci. Explor. 17 (1), 37–71.

Fukunnaga, K., 1991. Introduction to Statistical Pattern Recognition. Academic Press, pp. 38–40.

Gao, Y., Chen, K., 2006. Development of a real-time single-frequency precise point positioning system and test results. In: ION GNSS 19th International Technical Meeting of Satellite Division, 26–29 September 2006, Fort Worth, TX.

Garcia, R., Crespon, F., Ducic, V., Lognonné, P., 2005. Three-dimensional ionospheric tomography of post-seismic perturbations produced by the Denali earthquake from GPS data. Geophys. J. Int. 163, 1049–1064.

Hamilton, D.C., Gloeckler, G., Ipavich, F.M., Studemann, W., Wilken, B., Kremser, G., 1986. Ring current development during the great geomagnetic storm of February. J. Geophys. Res. 93, 14343.

Hegai, V.V., Kim, V.P., Nikiforova, L.I., 1997. A possible generation mechanism of acoustic-gravity waves in the ionosphere before strong earthquakes. J. Earthquake Predict. Res. 6, 584–589.

Hegai, V.V., Kim, V.P., Liu, J.Y., 2006. The ionospheric effect of atmospheric gravity waves excited prior to strong earthquake. Adv. Space Res. 37, 653–659.

Hernández-Pajares, M., Juan, J.M., Sanz, J., Orus, R., Garcia-Rigo, A., Feltens, J., Komjathy, A., Schaer, S.C., Krankowski, A., 2009. The IGS VTEC maps: a reliable source of ionospheric information since 1998. J. Geod. 83, 263–275. http://dx.doi.org/10.1007/s00190-008-0266-1.

Hobara, Y., Parrot, M., 2005. Ionospheric perturbations linked to a very powerful seismic event. J. Atmos. Solar Terr. Phys. 67, 677–685.

Jeong, D.H., Ziemkiewicz, C., Ribarsky, W., Chang, R., 2009. Understanding principal component analysis using a visual analytics tool. charlotte visualization center, UNC Charlotte.

Jin, S., Zhu, W., Afraimovich, E., 2010. Co-seismic ionospheric and deformation signals on the 2008 magnitude 8.0 Wenchuan Earthquake from GPS observations. Int. J. Remote Sens. 31 (13), 3535–3543.

Kechine, M.O., Tiberius, C.C.J.M., van der Marel, H., 2004. Real-time kinematic positioning with NASA's global differential GPS system. In: GNSS Conference, St. Petersburg, Russia.

Konga, H., Wang, L., Teoh, E.K., Li, X., Wang, J.G., Venkateswarlu, R., 2005. Generalized 2D principal component analysis for face image representation and recognition. Neural Networks 18, 585–594.

Kramer, M.A., 1991. Nonlinear principal component analysis using autoassociative neural networks. AIChE J. 37 (2), 233–243.

Lin, J.W., 2010. Ionospheric total electron content (TEC) anomalies associated with earthquakes through Karhunen–Loéve transform (KLT). Terr. Atmos. Oceanic Sci. 21, 253–265.

Lin, J.W., 2011. Use of principal component analysis in the identification of the spatial pattern of an ionospheric total electron content anomalies after China's May 12, 2008, M = 7.9 Wenchuan earthquake. Adv. Space Res. 47, 1983. http://dx.doi.org/10.1016/j.asr.2011.01.013.

Liu, J.Y., Chuo, Y.J., Shan, S.J., Tsai, Y.B., Pulinets, S.A., Yu, S.B., 2004. Pre-earthquake ionospheric anomalies monitored by GPS TEC. Ann. Geophys. 22, 1585–1593.

Liu, J.Y., Chen, Y.I., Chuo, Y.J., Chen, C.S., 2006. A statistical investigation of pre-earthquake ionospheric anomaly. J. Geophys. Res. 111, A05304, 10.1029/ 2005JA011333.

Liu, J.Y., Chen, Y.I., Chen, C.H., Liu, C.Y., Chen, C.Y., Nishihashi, M., Li, J.Z., Xia, Y.Q., Oyama, K.I., Hattori, K., Lin, C.H., 2009. Seismoionospheric GPS total electron content anomalies observed before the 12 May 2008 M_w = 7.9 Wenchuan earthquake. J. Geophys. Res. 114. http://dx.doi.org/10.1029/2008JA013698.

Liu, J.Y., Chen, C.H., Lin, C.H., Tsai, H.F., Chen, C.H., Kamogawa, M., 2011. Ionospheric disturbances triggered by the 11 March 2011 M9.0 Tohoku earthquake. J. Geophys. Res. 116, A06319. http://dx.doi.org/10.1029/2011JA016761.

Lognonné, P., Artru, J., Garcia, R., Crespon, F., Ducic, V., Jeansou, E., Occhipinti, G., Helbert, J., Moreaux, G., Godet, P.E., 2006. Ground-based GPS imaging of ionospheric post-seismic signal. Planet. Space Sci. 54, 528–540.

Marchand, R., Berthelier1, J.J., 2008. Simple model for post seismic ionospheric disturbances above an earthquake epicentre and along connecting magnetic field lines. Nat. Hazards Earth Syst. Sci. 8, 1341–1347.

Molchanov, O.A., Hayakawa, M., 1998. Subionospheric VLF signal perturbations possibly related to earthquakes. J. Geophys. Res. 103 (8), 17489–17504.

Mukherjee, G.K., 1999. Storm-associated variations of [OI] 630.0 nm emissions from low latitudes. Terr. Atmos. Oceanic. Sci. 10 (1), 265–276.

Ouyang, G., Wang, J., Wang, J., Cole, D., 2008. Analysis on temporal-spatial variations of Australian TEC. In: International Association of Geodesy Symposia, vol. 133, Part 4, pp. 751–758. http://dx.doi.org/10.1007/978-3-540-85426-5_86.

Pulinets, S.A., 2004. Ionospheric precursors of earthquakes; recent advances in theory and practical applications. Terr. Atmos. Oceanic Sci. 15 (3), 413–435.

Pulinets, S., Boyarchuk, K., 2004. Ionospheric Precursors of Earthquakes. Springer-Verlag, Berlin, Heidelberg.

Pulinets, S.A., Legen'ka, A.D., 2003. Spatial-temporal characteristics of the large scale disturbances of electron concentration observed in the F-region of the ionosphere before strong earthquakes. Cosmic Res. 41, 221–229.

Pulinets, S.A., Boyarchuk, K.A., Hegai, V.V., Kim, V.P., Lomonosov, A.M., 2000. Quasielectrostatic model of atmosphere–thermosphere ionosphere coupling. Adv. Space Res. 26 (8), 1209–1218.

Pulinets, S.A., Kotsarenko, N., Ciraolo, L., Pulinets, I.A., 2007. Special case of ionospheric day-to-day variability associated with earthquake preparation. Adv. Space Res. 39 (5), 970–977.

Sanguansat, P., 2012. Principal Component Analysis, InTech, Janeza Trdine 9, 51000 Rijeka, Croatia, 300pp.

Singh, R.P., Mehdi, W., Gautam, R., Senthil Kumar, J., Zlotnick, J., Kafatos, M., 2010. Precursory signals using satellite and ground data associated with the Wenchuan Earthquake of 12 May 2008. Int. J. Remote Sens. 31 (13), 3341–3354.

Yang, J., Zhang, D., Frangi, A.F., Yang, J.Y., 2004. Two-dimensional PCA: a new approach to appearance-based face representation and recognition. IEEE Trans. Pattern Anal. Mach. Intell. 26 (1), 131–137.

Zhao, B., Yu, T., Wang, M., Wan, W., Lei, J., Liu, L., Ning, B., 2008. Is an unusual large enhancement of ionospheric electron density linked with the 2008 great Wenchuan earthquake? J. Geophys. Res. 113, A11304. http://dx.doi.org/10.1029/2008JA013613.